

Determination of the magnetic order and the crystal symmetry in the multiferroic ground state of $\text{Ba}_2\text{CoGe}_2\text{O}_7$

V. Hutanu,^{1,*} A. Sazonov,² M. Meven,³ H. Murakawa,⁴ Y. Tokura,^{4,5,6} S. Bordács,^{4,7} I. Kézsmárki,⁷ and B. Náfrádi⁸

¹*Institut für Kristallographie, RWTH Aachen University, Outstation at FRM II, Garching, Germany*

²*CEA, Centre de Saclay; DSM/IRAMIS/Laboratoire Léon Brillouin, F-91191 Gif-sur-Yvette, France*

³*Forschungs-Neutronenquelle Heinz Maier-Leibnitz (FRM II) TU München, Garching, Germany*

⁴*Multiferroics Project, ERATO, Japan Science and Technology Agency (JST), University of Tokyo, Tokyo 113-8656, Japan*

⁵*Department of Applied Physics, University of Tokyo, Tokyo 113-8656, Japan*

⁶*Cross-Correlated Materials Group (CMRG) and Correlation Electron Research Group (CERG),*

RIKEN Advanced Science Institute, Wako 351-0198, Japan

⁷*Department of Physics, Budapest University of Technology and Economics and Condensed Matter Research Group of the Hungarian Academy of Sciences, 1111 Budapest, Hungary*

⁸*Max-Planck-Institut für Festkörperforschung, Heisenbergstraße 1, D-70569 Stuttgart, Germany*

(Received 14 May 2012; published 4 September 2012)

Detailed structural investigation of $\text{Ba}_2\text{CoGe}_2\text{O}_7$ was performed in its low-temperature multiferroic state combining neutron diffraction with magnetization measurements and the optical study of lattice vibrations on single crystals. The crystal structure above (10.4 K) and the crystal and magnetic structures below (2.2 K) the antiferromagnetic transition temperature of $T_N = 6.7$ K were determined using neutron diffraction. The tetragonal space group (SG) $P-42_1m$, corresponding to the average structure at room temperature, was found to also describe the structure at low temperatures well. Neutron diffraction data and infrared phonon mode analysis imply no structural phase transition down to 2.2 K. Orthorhombic polar SG $Cmm2$ is proposed as a true crystal structure. Below T_N , the spins of the Co^{2+} ions form a square-lattice Néel order within the (a,b) plane, while their alignment is ferromagnetic along the c axis. The magnitude of the ordered moment, fully lying within the (a,b) plane, is found to be $2.9(1) \mu_B/\text{Co}^{2+}$ and the easy axis of the sublattice magnetizations corresponds to the $[110]$ direction. A noncollinear spin structure due to small canting is allowed.

DOI: [10.1103/PhysRevB.86.104401](https://doi.org/10.1103/PhysRevB.86.104401)

PACS number(s): 75.85.+t, 75.50.Ee, 61.05.fm, 61.66.-f

I. INTRODUCTION

Study of multiferroics, materials simultaneously having more than one primary ferroic order parameter, is a hot topic of material sciences. The most extensively studied class of these compounds is the family of magnetoelectric multiferroics, where ferroelectricity can be induced by various types of magnetic orderings via the relativistic spin-orbit interaction.¹⁻³ As a consequence of the cross coupling between spins and electric polarization, the spectacular control of the ferroelectric polarization by external magnetic field and the manipulation of the magnetic order via electric field can often be realized in these systems. Thus, multiferroics are interesting for potential use in spintronics and data storage. Though the basic symmetry requirements for the existence of magnetoelectric cross coupling are well known, the microscopic mechanisms and spin textures responsible for this phenomenon need to be clarified in order to optimize the synthesis of multiferroics.

Recently, $\text{Ba}_2\text{CoGe}_2\text{O}_7$ has attracted significant scientific interest due to its peculiar magnetoelectric behavior^{4,5} and its giant directional dichroism in resonance with both electrically and magnetically active spin excitations located in the terahertz region.⁶ In Ref. 4, spontaneous electric polarization along the $[001]$ direction (EPc) is reported below the magnetic transition temperature of $T_N = 6.7$ K in zero external field. Weak ferromagnetism was observed below T_N by Refs. 5 and 7 and was proposed to be an intrinsic characteristic of the magnetic order as a result of the small noncollinear canting of the spin moment. As a variant, in Ref. 8, it is assumed that the magnetic structure is nearly collinear (with a canting

angle less than 0.1°) in the zero-applied field and becomes canted by applying an external field. The delicate control of the ferroelectricity via the direction of an external magnetic field has also been demonstrated by Ref. 5. The ferroelectric polarization along the c axis and the a axis were found to oscillate with a periodicity of 180° when rotating the magnetic field within the (a,b) and (b,c) planes, respectively. These features have been successfully described by a spin-dependent metal-ligand $p-d$ hybridization mechanism.^{5,8} Very recently, a theoretical analysis solely based on symmetry arguments has shown that the main features of the magnetoelectric behavior of $\text{Ba}_2\text{CoGe}_2\text{O}_7$ can be predicted and understood without appealing to any particular atomic mechanism.⁹ Besides the dc magnetoelectric phenomena, the theory of unusual spin excitations and the corresponding optical magnetoelectric effects in $\text{Ba}_2\text{CoGe}_2\text{O}_7$ has been developed in Refs. 10 and 11. The onset of spontaneous toroidal moment in the multiferroic phase of $\text{Ba}_2\text{CoGe}_2\text{O}_7$ has been argued to play a crucial role in the magnetoelectric phenomena.¹²

It is clear that precise structural information both for the nuclei and about the spin order (crystal and magnetic structures) is essential to unravel the complex physics behind the magnetoelectric behavior of the compound. Nevertheless, detailed structural investigation of $\text{Ba}_2\text{CoGe}_2\text{O}_7$ at low temperatures has not been done yet. In each theoretical work mentioned above, it was assumed that $\text{Ba}_2\text{CoGe}_2\text{O}_7$ is isostructural with $\text{Ca}_2\text{CoSi}_2\text{O}_7$ and has the melilite-type $P-42_1m$ symmetry space group (SG, No. 113)¹³ referring to a previous report of Zheludev *et al.*¹⁴ However, in Ref. 14, the

lattice structure of $\text{Ba}_2\text{CoGe}_2\text{O}_7$ was not investigated; instead, it was treated as a line compound of $\text{Ba}_2\text{Cu}_x\text{Co}_{1-x}\text{Ge}_2\text{O}_7$ solid solutions and was assumed to be isostructural with $\text{Ba}_2\text{CuGe}_2\text{O}_7$. A preliminary magnetic structure refinement in $\text{Ba}_2\text{CoGe}_2\text{O}_7$ at 3.5 K by neutron diffraction on a triple axis spectrometer using a large mosaic sample was performed.¹⁴ The lack of the crystallographic data necessary to bring the measured magnetic intensities of the 19 nonequivalent Bragg reflections to an absolute scale did not allow the determination of the magnitude of the ordered moment. Moreover, the limitation of the dataset to one scattering plane ($h, 0, l$) only allowed an approximate determination of the spin structure. The authors concluded that $S = 3/2$ spins of the Co ions form a square lattice antiferromagnetic state within the (a, b) plane, with magnetic moments lying within these planes, while the alignment of neighboring spins along the c axis is ferromagnetic.

Recently, a detailed crystal structure determination of $\text{Ba}_2\text{CoGe}_2\text{O}_7$ was performed at room temperature (RT) and at 90 K¹⁵ using synchrotron radiation. The characteristic SG for melilite-type compounds $P-42_1m$ was confirmed to describe the average structure at the studied temperatures well. However, as follows from the observation of a set of superstructure reflections violating the 2_1 symmetry, the real structure of $\text{Ba}_2\text{CoGe}_2\text{O}_7$ is more distorted and has a lower symmetry. One has to note that these superstructure reflections appear at \mathbf{Q} vectors in the reciprocal space where the magnetic Bragg peaks in neutron diffraction occurs below $T_N = 6.7$ K.¹⁴ Symmetry analysis¹⁵ showed two possible SG candidates for the true structure: tetragonal $P-4$ (No. 81)¹³ and orthorhombic $Cmm2$ (No. 35).¹³ It is known that many of the melilite-like compounds (e.g. $\text{Ca}_2\text{CoSi}_2\text{O}_7$) may show at lower temperatures incommensurate or commensurate modulated lock-in phases.¹⁶ The question whether $\text{Ba}_2\text{CoGe}_2\text{O}_7\text{O}$ at low temperature has the same structure as at room temperature or 90 K is still an open issue.

In order to determine the structural parameters of $\text{Ba}_2\text{CoGe}_2\text{O}_7$ and to fully characterize its magnetic order in the multiferroic state, we performed a detailed crystallographic study at temperatures just above and below the magnetic phase transition by neutron diffraction on single crystals. Magnetic symmetry analysis and bulk magnetization measurements were used for selecting the model for the refinement of the neutron diffraction data. The IR reflectivity spectra measurements of the optical phonon modes were performed for different light polarizations at various temperatures as an additional method to evidence a possible structural phase transition related to the magnetic ordering. These results provide a solid basis to understand the microscopic origin of the magnetoelectricity in $\text{Ba}_2\text{CoGe}_2\text{O}_7$.

II. EXPERIMENTAL

High-quality single-crystal $\text{Ba}_2\text{CoGe}_2\text{O}_7$ was grown using a floating zone method similarly to those used in previous studies.^{5,6} The sample used in the present neutron diffraction experiments is a $\frac{1}{4}$ segment of a disc with a diameter of 5 mm and a thickness of 2 mm. It is a part of a larger crystal from which other pieces were studied with synchrotron x-ray diffraction.¹⁵ This sample was studied at the neutron

source Heinz Maier-Leibnitz (FRM II) on the hot four circle diffractometer HEiDi.¹⁷ Using a Cu-(220) monochromator, one obtains a short wavelength of 0.87 Å with a high flux density of $>4.5 \times 10^6$ neutrons $\text{s}^{-1}\text{cm}^{-2}$. The extinction as a typical source of systematic errors is negligible small at this wavelength. The sample was placed into an He closed-cycle cryostat and mounted in the Eulerian cradle of the diffractometer. The crystal was wrapped in Al foil in order to improve the homogeneity of the temperature. The temperature was measured and controlled by a diode sensor near the sample position with a stability of ± 0.1 K. The correction of the measured integrated intensities was performed using the program PRON2K10.¹⁸ The program MAGLSQ of the Cambridge Crystallography Subroutine Library¹⁹ was used to refine the parameters of the nuclear and magnetic structures. Full details of the structural refinements are available as crystallographic information files (CIF).²⁰

The angular dependence of the magnetization was measured in a 7-T superconducting magnet equipped with a dc magnetometer. During the experiment, the sample was rotated around the [001] axis being perpendicular to the magnetic field, and the magnetization parallel to the applied field was detected. The initial direction of the single crystal was set under an optical microscopy by about 5° precision. The direction was changed by pulling the string which was tied to the rotation axis of the sample stage. This procedure allows a control of the sample orientation by about 1° precision.

The polarized optical reflectivity measurements over the far infrared region were carried out using a Bruker IFS-66 Fourier transform spectrometer. The samples were mounted on the cold finger of a He-flow optical cryostat.

III. RESULTS

We used bulk magnetization (M) measurements to determine the direction of the easy axis of the magnetization. In Ref. 7, the temperature dependence of the magnetization in fields $H = 0.1$ T parallel and perpendicular to the (a, b) plane demonstrate a strong anisotropy between these two directions at low temperatures. The magnetization within the (a, b) plane is twice as large as perpendicular to it in accordance with the easy-plane AFM state determined from neutron scattering. The angular dependence of M in the (a, b) plane was investigated only in larger field ($H = 1$ T) earlier,⁵ where the magnetization can be freely rotated in the tetragonal plane with negligible modulation.⁵ In Fig. 1, the experimental results of the in-plane H -rotation measurement and the observed angular dependence at $T = 2$ K are shown in small fields of $H = 0.1$ and 0.3 T. Clear oscillations of the magnetization with an almost pure 180° period, characteristic to orthorhombic symmetry, were found. Please note that $H = 0.3$ T is more than three times larger than the coercive field. Therefore, the angular dependence reflects the in-plane magnetic anisotropy experienced during the rotation of a single domain.

It has been found in several insulator magnets that the change in the dynamical properties of the lattice upon a magnetic transition reflects the magnetically induced crystal symmetry lowering more clearly than the static distortions.²¹⁻²³ To address the question of orthorhombic distortion the temperature dependence of the infrared active phonon modes

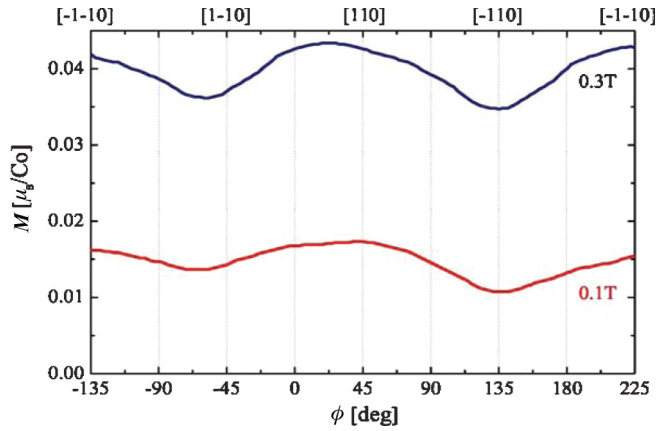


FIG. 1. (Color online) The angular dependence of the magnetization M in the (001) plane. ϕ is the angle between [100] and H .

across the magnetic transition were studied. The left and right panels of Fig. 2 show the far infrared reflectivity spectra for light polarization parallel and perpendicular to the (a,b) plane, respectively. We could assign each of the 10 B_2 modes expected in the tetragonal SG $P-42_1m$ and 17 E modes out of the total 18, though some of them correspond to weak features in the reflectivity spectra. The phonon frequencies for the B_2 modes are $\omega = 130, 150, 180, 226, 277, 380, 410, 460, 490,$ and 770 cm^{-1} , while the E modes are $\omega = 70, 95, 107, 152, 165, 185, 225, 255, 277, 315, 405, 420, 467, 503, 700, 770,$ and 858 cm^{-1} . The lack of resonances common for both polarizations ensures the proper orientation and the single-domain nature of the crystal.

Prior to the studies of the $\text{Ba}_2\text{CoGe}_2\text{O}_7$ magnetic structure, the crystal structure was measured at 10.4 K, just above $T_N = 6.7 \text{ K}$ by neutron diffraction. A total number of 582 Bragg reflections with $\sin\theta/\lambda \leq 0.7 \text{ \AA}^{-1}$ were collected. The number of reflections satisfying the criterion $I > 2\sigma(I)$, used for the refinement was 525. The magnetic structure of $\text{Ba}_2\text{CoGe}_2\text{O}_7$ was investigated at 2.2 K. A total number of 571 nuclear and magnetic Bragg reflections with $\sin\theta/\lambda \leq 0.7 \text{ \AA}^{-1}$ were measured. The number of the reflections satisfying the criterion $I > 2\sigma(I)$ and used for the refinement was 522.

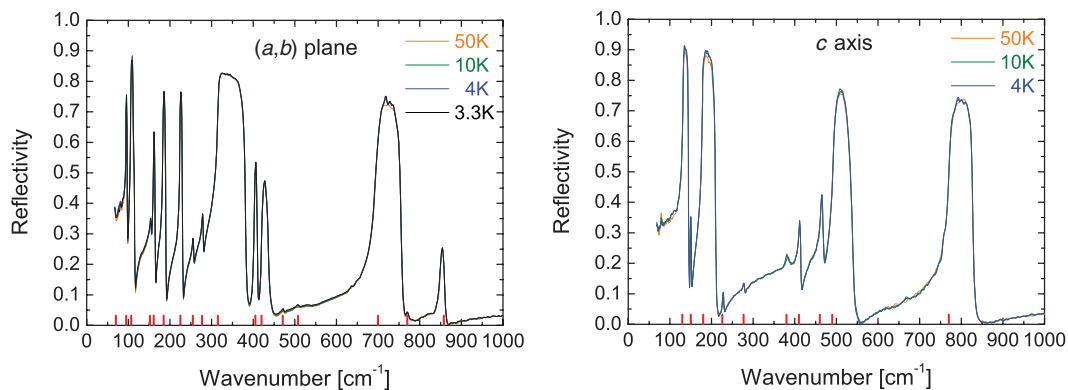


FIG. 2. (Color online) Reflectivity spectra of $\text{Ba}_2\text{CoGe}_2\text{O}_7$ in the region of optical phonon modes ($65\text{--}1000 \text{ cm}^{-1}$) at various temperatures. Left/right panel: Infrared active phonon modes for polarization within/perpendicular to the (a,b) plane. The positions of the modes are indicated by red vertical bars.

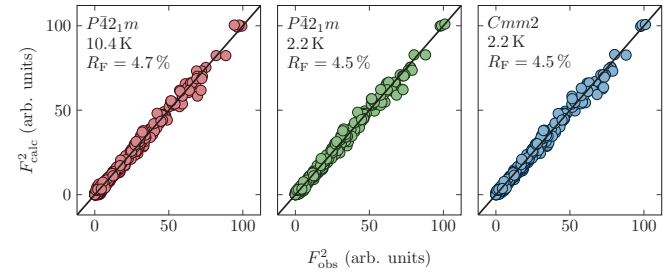


FIG. 3. (Color online) Quality of the diffraction data refinement both for the nuclear and the magnetic structure of $\text{Ba}_2\text{CoGe}_2\text{O}_7$. The experimental integrated intensities (F_{obs}^2) are plotted against the calculated ones (F_{calc}^2). Left panel: Nuclear intensities at 10.4 K for SG $P-42_1m$. Middle panel: Both nuclear and magnetic intensities at 2.2 K refined for the nuclear SG $P-42_1m$. Right panel: Both nuclear and magnetic intensities at 2.2 K refined for the nuclear SG $Cmm2$.

Starting parameters for the least-squares refinement were obtained from the average structure determined previously in the tetragonal SG $P-42_1m$ at 90 K by synchrotron x-ray single-crystal diffraction.¹⁵ The quality of the fit, assuming the paramagnetic average tetragonal SG $P-42_1m$, is shown in the left panel of Fig. 3. We performed refinement of the magnetic structure in the orthorhombic MSG $Cm'm2'$. In the first step of the refinement, the nuclear structure parameters were fixed at the experimental values obtained at 10.4 K, while in the final step, both nuclear and magnetic structures were refined simultaneously. In addition to the nuclear parameters, the magnitude of the Co magnetic moment and the canting angle ϕ' between its direction and [110] in the (a,b) plane were refined. In the middle panel of Fig. 3, the quality of the fit based on the orthorhombic MSG $Cm'm2'$ SG is shown.

IV. DISCUSSIONS

Almost pure 180° period oscillations of the magnetization were found at $T = 2 \text{ K}$ at both 0.1 and 0.3 T in-plane fields (Fig. 1). This periodicity is an indication for an orthorhombic symmetry. The maximum magnetization is seen with a field pointing to $\phi = 45^\circ$ (ϕ is the angle between [100] and the applied field). Therefore, one can identify [110] as the easy

axis of the magnetization with the canted component of the magnetization parallel to it.

We investigated the temperature dependence of the phonon spectra across the magnetic transition from 50 K down to 3.3 K (Fig. 2). In the tetragonal SG $P-42_1m$, the factor group analysis yields 28 infrared active phonon modes. Among them, 18 E modes are twofold degenerate and excited by light polarized within the (a,b) plane, while 10 B_2 modes are nondegenerate and active for polarization along the c axis. In case the lattice symmetry is lowered to orthorhombic, lifting of the twofold degeneracy should be observed for the E modes.

The reflectivity spectra measured at different temperatures are identical within the precision of the experiment for both polarizations (Fig. 2). The weakness of the temperature-induced sharpening and red shift of the modes indicate negligible thermal expansion below 50 K. No splitting of the E modes, i.e. no supplementary orthorhombic distortion, related to the magnetic phase transition at 6.7 K, could be detected within the resolution of the experiment corresponding to $\delta = 0.5 \text{ cm}^{-1}$ or 0.06 meV.

It was shown¹⁵ that the true structure of $\text{Ba}_2\text{CoGe}_2\text{O}_7$ is either tetragonal $P-4$ or orthorhombic $Cmm2$. However, the distortions which lead to the symmetry lowering are found to be extremely small. Correspondingly, the refinements of the structural parameters within either of the two subgroups do not change the quality of the fit towards any direction, which could allow us to exclude one of the two proposed SG candidates. Under these circumstances one may conclude that, within the error of the experiment, tetragonal $P-42_1m$ SG (No. 113)¹³ is a very good approximation of the average nuclear structure of $\text{Ba}_2\text{CoGe}_2\text{O}_7$ at 10.4 K (paramagnetic phase). Table I shows the fractional atomic coordinates and the isotropic atomic displacement parameters (ADPs) of the crystal structure of $\text{Ba}_2\text{CoGe}_2\text{O}_7$ determined in $P-42_1m$ SG at 10.4 K. The quality of the fit is shown in the left panel of Fig. 3.

As shown by Perez-Mato and Ribeiro⁹ and also by Bordács *et al.*,¹¹ the AFM ordering in this material breaks the paramagnetic space group $P-42_1m1'$ into different magnetic space groups (MSG) depending on the orientation of the sublattice magnetizations. For the AFM component of the sublattice magnetizations lying along the direction [100] (as proposed to be the ground state in Ref. 14) the resulting MSG is $P2'_12_12'_1$. For the AFM spin configuration along [110] (as suggested to be the ground state, e.g. in Ref. 5) the resulting MSG is $Cm'm2'$. For a more general direction of the spins in the (a,b) plane the symmetry reduces to $P112'_1$. For the symmetry-related orientations, e.g. [010] and $[-110]$,

$P2'_12_12'_1$ and $Cmm'2'$ are realized, which form energetically equivalent domains of the same equilibrium phase. In an applied magnetic field, the magnetic point-group symmetry of the system changes as a function of the field orientation among the different magnetic space groups mentioned above.⁹ In zero magnetic field, it is impossible to distinguish between $P2'_12_12'_1$, $Cm'm2'$, and $P112'_1$ with conventional neutron diffraction due to the presence of the magnetic domains in each case. Measurements of macroscopic quantities, such as the bulk magnetization and ferroelectric polarization, can help to clarify this point in combination with the information from the present neutron scattering data. The magnetic space group $P2'_12_12'_1$ in the zero-field ground state can be ruled out, as it does not allow a spontaneous polarization along z , which is observed experimentally in $\text{Ba}_2\text{CoGe}_2\text{O}_7$.⁴ Moreover, as was shown by Toledano *et al.*,¹² the phase which corresponds to $P112'_1$ cannot be reached directly from the paramagnetic state if the phase transition at T_N is a second-order one. Therefore, the phase with the magnetic symmetry $Cm'm2'$, which displays four magnetic domains, can be identified as the magnetic phase of $\text{Ba}_2\text{CoGe}_2\text{O}_7$ below T_N .

The results on the angular dependence of the magnetization and the symmetry arguments above give clear motivation to perform a refinement of the magnetic structure in the orthorhombic MSG $Cm'm2'$. The quality of the fit shows (Fig. 3, middle panel) that the chosen model describes the nuclear and magnetic structure accurately. The refined fractional atomic coordinates and isotropic ADPs of the crystal structure of $\text{Ba}_2\text{CoGe}_2\text{O}_7$ determined in SG $P-42_1m$ at 2.2 K are presented in Table II. The results show no significant difference between the structure above and below the magnetic transition. All the fractional atomic coordinates at 2.2 K remain the same as for 10.4 K within the error bars. Thus, no evidence of structural phase transition associated with the magnetic ordering is observed, although the 180° periodicity of the magnetization implies that the crystal structure is orthorhombic. Assuming that the magnetic phase transition at $T_N = 6.7$ K is a second-order transition and lattice distortion is coupled to the magnetic order parameter, a 90° periodicity of the magnetization would be expected in case of $P-42_1m$ symmetry in the paramagnetic phase. Thus, either the crystal symmetry might already be orthorhombic in the paramagnetic phase or the transition is of weakly first order.

The magnetic structure of $\text{Ba}_2\text{CoGe}_2\text{O}_7$ ($Cm'm2'$ domain) is illustrated in Fig. 4. This magnetic space group allows a spin canting, i.e. an FM component within the (a,b) plane, perpendicular to the direction of the primary AFM

TABLE I. Nuclear structure parameters of $\text{Ba}_2\text{CoGe}_2\text{O}_7$ at 10.4 K in $P-42_1m$.

Wyckoff		X	Y	Z	$U_{\text{iso}}/U_{\text{eqv}}$
Ion	position				
Ba	4e	0.33465(14)	0.16537(14)	0.49239(28)	0.0010(3)
Co	2b	0	0	0	0.0023(9)
Ge	4e	0.14085(11)	0.35915(11)	0.04031(19)	0.0027(2)
O1	2c	0	0.5	0.15996(39)	0.0044(4)
O2	4e	0.13802(16)	0.36200(16)	0.72960(27)	0.0044(3)
O3	8f	0.07906(15)	0.18452(14)	0.18825(20)	0.0043(2)

TABLE II. Nuclear structure parameters of $\text{Ba}_2\text{CoGe}_2\text{O}_7$ at 2.2 K in $P-42_1m$.

Wyckoff		X	Y	Z	$U_{\text{iso}}/U_{\text{eqv}}$
Ion	position				
Ba	4e	0.33466(16)	0.16536(16)	0.49235(29)	0.0009(3)
Co	2b	0	0	0	0.0017(9)
Ge	4e	0.14073(12)	0.35927(12)	0.04019(20)	0.0023(2)
O1	2c	0	0.5	0.15942(43)	0.0040(5)
O2	4e	0.13793(17)	0.36209(17)	0.72955(29)	0.0041(3)
O3	8f	0.07906(16)	0.18446(16)	0.18857(21)	0.0042(2)

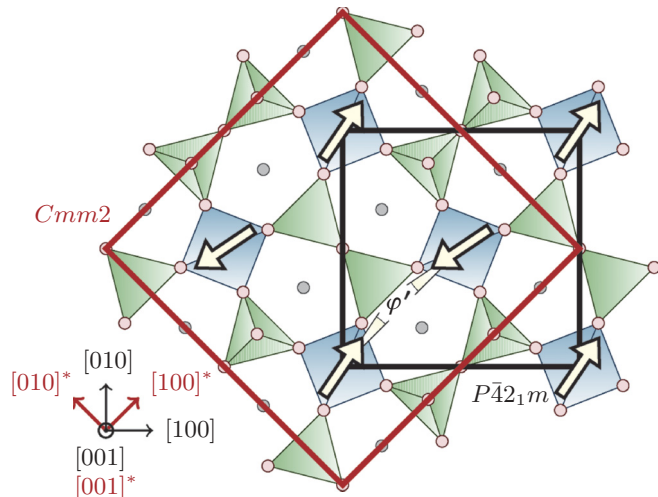


FIG. 4. (Color online) Magnetic structure of $\text{Ba}_2\text{CoGe}_2\text{O}_7$ at 2.2 K: View along the $[001]$ direction. Both $P\bar{4}2_1m$ and $Cmm2$ crystallographic unit cells are shown.

ordering.⁹ Due to the small number of solely magnetic Bragg reflections, which are rather weak as compared with the nuclear scattering intensities, the canting angle could not be determined with high precision. More importantly, the population of the four possible magnetic domains strongly affects the value of the canting angle obtained from the refinement of the available data. Polarized neutron diffraction experiments in the monodomain sample are needed to unambiguously determine the canting angle. Along the c axis, the moments are ordered ferromagnetically. Taking into account the melilite-like layered structure, the main magnetic interactions are expected to occur in the (a,b) plane. The strong 2D character of the magnetism in $\text{Ba}_2\text{CoGe}_2\text{O}_7$ was also confirmed by the magnetization measurement.⁷ As an important result of the present neutron scattering study, the magnitude of the ordered magnetic moment of Co ions could be refined with high accuracy to be $2.9 \pm 0.1 \mu_B$.

A previous study¹⁵ showed that the true structure of $\text{Ba}_2\text{CoGe}_2\text{O}_7$ should have either the tetragonal SG $P\bar{4}$ or the orthorhombic SG $Cmm2$. Considering the following, one might exclude the tetragonal SG $P\bar{4}$: (a) a magnetic structure generally follows the crystal symmetry; (b) the evidence of the orthorhombicity is present in the magnetization data as seen in Fig. 1; (c) the good result of the refinement of the magnetic structure for the orthorhombic MSG $Cm'm'2'$; and (d) no evidence of a structural transition is provided either by neutron scattering or by infrared phonon analysis. Under these circumstances the refinement of the available data in SG $Cmm2$ gives the structural parameters of the true structure of $\text{Ba}_2\text{CoGe}_2\text{O}_7$. In the right panel of Fig. 3, the quality of the diffraction data refinement for both nuclear and magnetic structures of $\text{Ba}_2\text{CoGe}_2\text{O}_7$ using $Cmm2$ SG and $Cm'm'2'$ MSG is shown. Table III presents the refined fractional atomic coordinates and isotropic ADPs of the crystal structure of $\text{Ba}_2\text{CoGe}_2\text{O}_7$ determined in SG $Cmm2$ at 2.2 K. The lattice constants of the true structure are $a = b = 11.803(4) \text{ \AA}$, $c = 5.500(19) \text{ \AA}$. The comparison between the average and true structure lattices is illustrated in the Fig. 4. We emphasize that both the quality of the diffraction data refinement and

TABLE III. Nuclear structure parameters of $\text{Ba}_2\text{CoGe}_2\text{O}_7$ at 2.2 K in SG $Cmm2$.

Ion	Wyckoff position	X	Y	Z	$U_{\text{iso}}/U_{\text{eqv}}$
Ba1	4d	0.33423(27)	0	0.4926(14)	0.0011(5)
Ba2	4e	0.5	0.66498(25)	0.5079(13)	0.0008(5)
Co	4c	0.25	0.75	0	0.0021(9)
Ge1	4d	0.14100(18)	0	0.0401(13)	0.0025(4)
Ge2	4e	0.5	0.85953(17)	0.9598(13)	0.0022(4)
O1	2a	0	0	0.1583(14)	0.0038(7)
O2	2b	0.5	0	0.8396(14)	0.0044(7)
O3	4d	0.13789(27)	0	0.7298(13)	0.0041(5)
O4	4e	0.5	0.86198(25)	0.2706(13)	0.0044(5)
O5	8f	0.19739(19)	0.88184(16)	0.1881(16)	0.0043(4)
O6	8f	0.38173(18)	0.80280(16)	0.8110(12)	0.0043(4)

the magnitude of the ordered moment are nonsensitive to the choice whether the tetragonal $P\bar{4}2_1m$ or the orthorhombic $Cmm2$ models of the crystal structure is used in the refinement.

Due to the lack of the structural parameters on $\text{Ba}_2\text{CoGe}_2\text{O}_7$, in a number of recent studies regarding the multiferroic behavior of the title compound, the crystal structure of the melilite-type compounds, like $\text{Ca}_2\text{CoSi}_2\text{O}_7$ (Refs. 5 and 8) or $\text{Ba}_2\text{CuGe}_2\text{O}_7$ (Ref. 14), has been used. It was found that $\text{Ca}_2\text{CoSi}_2\text{O}_7$ forms incommensurate or commensurate modulated lock-in phases at the low temperatures,¹⁶ while $\text{Ba}_2\text{CuGe}_2\text{O}_7$ has an incommensurate magnetic structure.²⁴ In contrast, no indications of incommensurability in the crystal and magnetic structure of $\text{Ba}_2\text{CoGe}_2\text{O}_7$ were found down to 2.2 K. Concerning the location of the magnetic Co ions, we emphasize that, in full agreement with former structural data, there is only one crystallographically independent Co ion occupying the $2b$ Wyckoff position (WP) in $P\bar{4}2_1m$ or $4c$ WP in $Cmm2$ structure.

In Table IV, the available data from the literature are presented regarding the lattice constants of $\text{Ba}_2\text{CoGe}_2\text{O}_7$ measured at different temperatures (all refined in the tetragonal SG $P\bar{4}2_1m$). Although the results for the lattice constants at room temperature in Refs. 15 and 25 were obtained using different diffraction methods—synchrotron radiation x-ray diffraction on a single crystal in Ref. 15 and laboratory x-ray powder diffraction in Ref. 25—the resulting values are in good agreement. At low temperature (10 K), the lattice constants, measured by single-crystal neutron diffraction in Ref. 14, differ from our results, although no error bars are specified for the lattice parameters in Ref. 14. We also note that our

TABLE IV. Lattice constants of $\text{Ba}_2\text{CoGe}_2\text{O}_7$ in $P\bar{4}2_1m$ SG at different temperatures

Temperature	a , \AA	c , \AA	Source
298 K	8.381(2)	5.554(15)	This paper
297 K	8.3836(3)	5.5510(3)	Ref. 25
293 K	8.3845(1)	5.5497(2)	Ref. 15
90 K	8.3802(1)	5.5435(1)	Ref. 15
10.4 K	8.346(3)	5.500(19)	This paper
10 K	8.410	5.537	Ref. 14

low-temperature lattice parameters are in good agreement with the high-temperature data (both ours and those from the literature) assuming linear-like thermal evolution.

V. CONCLUSIONS

The magnetic structure of $\text{Ba}_2\text{CoGe}_2\text{O}_7$ at 2.2 K was accurately refined from the neutron diffraction data using the magnetic symmetry analysis from Refs. 9 and 12 and original experimental data on the angular dependence of the magnetization in the (a,b) plane. The results indicate the orthorhombic symmetry of the magnetic structure with MSG $Cm'm2'$. The spin pattern shows a square-lattice AFM order within the (a,b) plane, while the alignment of the spins is ferromagnetic along the c axis. The magnitude of the ordered magnetic moment of Co^{2+} ions is found to be $2.9 \pm 0.1 \mu_B$, and the easy axis of the sublattice magnetizations corresponds to [110]. Small canting leading to the existence of the tiny spontaneous magnetization in the (a,b) plane below T_N is allowed according to the magnetic symmetry and neutron diffraction data.

No evidence for a structural phase transition upon the magnetic phase transition at 6.7 K was observed either by neutron diffraction or in the lattice dynamics. Taking into account the orthorhombic symmetry of the magnetic structure (MSG $Cm'm2'$) and the fact that no structural phase transition has been observed, one could assume that the true structure of

$\text{Ba}_2\text{CoGe}_2\text{O}_7$ is also orthorhombic. This assumption is indeed supported by a previous synchrotron investigation,¹⁵ where the SG $Cmm2$ was suggested as one of the two possible true structures in the paramagnetic state of $\text{Ba}_2\text{CoGe}_2\text{O}_7$. This is the same symmetry as the one found for the magnetic structure, except for the addition of the time reversal. We also report here the structural parameters for this true structure of $\text{Ba}_2\text{CoGe}_2\text{O}_7$ in the AFM (multiferroic) phase.

The melilite-type tetragonal SG ($P-42_1m$), widely accepted as the average structure at room temperature, describes accurately the low-temperature structure of $\text{Ba}_2\text{CoGe}_2\text{O}_7$, both above and below the AFM transition. Here, we also report the structural parameters for this average structure in the paramagnetic and AFM state.

The reported structural parameters (both for the nuclear and magnetic order) can serve as a profound experimental basis to develop microscopic models describing the multiferroic nature and the peculiar magnetoelectric phenomena of $\text{Ba}_2\text{CoGe}_2\text{O}_7$.

ACKNOWLEDGMENTS

We thank G. Heger for fruitful discussions. This work was partly supported by the German DFG (Grant No. SFB/TRR 80) and BMBF (Contract No. 05K10PA2). This work was partly supported by Hungarian OTKA under Grant Nos. PD75615, CNK80991, Bolyai program, TÁMOP-4.2.2/B-10/1/-2010-0009.

*Corresponding author: vladimir.hutaniu@frm2.tum.de

¹M. Fiebig, *J. Phys. D: Appl. Phys.* **38**, R123 (2005).

²K. F. Wang, J. M. Liu, and Z. F. Ren, *Adv. Phys.* **58**, 321 (2009).

³S. W. Cheong and M. Mostovoy, *Nat. Mater.* **6**, 13 (2007).

⁴H. T. Yi, Y. J. Choi, S. Lee, and S.-W. Cheong, *Appl. Phys. Lett.* **92**, 212904 (2008).

⁵H. Murakawa, Y. Onose, S. Miyahara, N. Furukawa, and Y. Tokura, *Phys. Rev. Lett.* **105**, 137202 (2010).

⁶I. Kézsmárki, N. Kida, H. Murakawa, S. Bordács, Y. Onose, and Y. Tokura, *Phys. Rev. Lett.* **106**, 057403 (2011).

⁷T. Sato, T. Masuda, and K. Uchinokura, *Phys. B* **329–333**, 880 (2003).

⁸K. Yamauchi, P. Barone, and S. Picozzi, *Phys. Rev. B* **84**, 165137 (2011).

⁹J. M. Perez-Mato and J. L. Ribeiro, *Acta Cryst. A* **67**, 264 (2011).

¹⁰S. Miyahara and N. Furukawa, *J. Phys. Soc. Jpn.* **80**, 073708 (2011).

¹¹S. Bordács, I. Kézsmárki, D. Szaller, L. Demkó, N. Kida, H. Murakawa, Y. Onose, R. Shimano, T. Rőöm, U. Nagel, S. Miyahara, N. Furukawa, and Y. Tokura, *arXiv:1109.1597*.

¹²P. Toledano, D. D. Khalyavin, and L. C. Chapon, *Phys. Rev. B* **84**, 094421 (2011).

¹³*International Tables for Crystallography*, edited by Th. Hahn, Vol. A (Springer, Dordrecht, 2005).

¹⁴A. Zheludev, T. Sato, T. Masuda, K. Uchinokura, G. Shirane, and B. Roessli, *Phys. Rev. B* **68**, 024428 (2003).

¹⁵V. Hutanu, A. Sazonov, H. Murakawa, Y. Tokura, B. Náfrádi, and D. Chernyshov, *Phys. Rev. B* **84**, 212101 (2011).

¹⁶Z. H. Jia, Ph.D. Thesis, University Marburg Germany, 2005.

¹⁷M. Meven, V. Hutanu, and G. Heger, *Neutron News* **18**, 19 (2007).

¹⁸Program for data reduction of DIF4. Version of the Institut für Kristallographie, RWTH Aachen.

¹⁹P. J. Brown and J. C. Matthewman, *The Cambridge Crystallography Subroutine Library Users' Manual* (2009), <http://www.ill.eu/sites/ccsl/html/ccsl/doc.html>.

²⁰ICSD, <http://www.fiz-karlsruhe.de>, structure at 10 K, 2.4 K (2012).

²¹T. Rudolf, Ch. Kant, F. Mayr, J. Hemberger, V. Tsurkan, and A. Loidl, *New J. Phys.* **9**, 76 (2007).

²²S. Bordács, D. Varjas, I. Kézsmárki, G. Mihály, L. Baldassarre, A. Abouelsayed, C. A. Kuntscher, K. Ohgushi, and Y. Tokura, *Phys. Rev. Lett.* **103**, 077205 (2009).

²³A. B. Sushkov, O. Tchernyshyov, W. Ratcliff II, S. W. Cheong, and H. D. Drew, *Phys. Rev. Lett.* **94**, 137202 (2005).

²⁴A. Zheludev, G. Shirane, Y. Sasago, N. Kiode, and K. Uchinokura, *Phys. Rev. B* **54**, 15163 (1996).

²⁵H. F. McMurdie, E. H. Evans, B. Paretzkin, W. Wong-Ng, and E. Etlinger, *Powder Diffr.* **1**(2), 64 (1986).